arXiv:1412.5280v2 [cond-mat.quant-gas] 24 Mar 2015

Polaronic atom-trimer continuity in three-component Fermi gases

Yusuke Nishida
Department of Physics, Tokyo Institute of Technology, Ookayama, Meguro, Tokyo 152-8551, Japan
(Dated: December 2014)

Recently it has been proposed that three-component Fermi gases may exhibit a new type of crossover physics in which an unpaired Fermi sea of atoms smoothly evolves into that of trimers in addition to the ordinary BCS-BEC crossover of condensed pairs. Here we study its corresponding polaron problem in which a single impurity atom of one component interacts with condensed pairs of the other two components with equal populations. By developing a variational approach in the vicinity of a narrow Feshbach resonance, we show that the impurity atom smoothly changes its character from atom to trimer with increasing the attraction and eventually there is a sharp transition to dimer. The emergent polaronic atom-trimer continuity can be probed in ultracold atoms experiments by measuring the impurity spectral function. Our novel crossover wave function properly incorporating the polaronic atom-trimer continuity will provide a useful basis to further investigate the phase diagram of three-component Fermi gases in more general situations.

PACS numbers: 67.85.Lm, 03.75.Ss, 11.10.St, 74.20.Fg

INTRODUCTION

Interacting Fermi systems appear across a broad range of physics with various interaction strengths and understanding of their properties is of fundamental importance. When there is a weak attraction between two components of fermions, the system is unstable toward the formation of Cooper pairs and becomes a Bardeen-Cooper-Schrieffer (BCS) superfluid. On the other hand, when the attraction is sufficiently strong, the two components of fermions form a diatomic molecule which undergoes the Bose-Einstein condensation (BEC) and the system becomes the superfluid again. Because there is no sharp distinction between the condensation of loosely bound Cooper pairs and tightly bound molecules, the above two types of superfluids can be smoothly connected with increasing the attraction. Indeed, it was shown that the ordinary mean-field wave function smoothly interpolates the BCS and BEC superfluids which constitutes the celebrated BCS-BEC crossover theory providing unified understanding of Fermi superfluids [1, 2]. Since then the BCS-BEC crossover in two-component Fermi gases has been the subject of extensive studies [3] and now recognized as a well-established phenomenon, in particular, because of its experimental realization with ultracold atoms utilizing Feshbach resonances [4–6].

Yet richer crossover physics may be found in three-component Fermi gases [7–9]. When an attraction between three components of fermions is weak, two of them form Cooper pairs and condense while there is always one component that remains unpaired and forms a Fermi sea [10–14]. Then, with increasing the attraction, loosely bound Cooper pairs will smoothly evolve into tightly bound molecules according to the BCS-BEC crossover. But, what will happen to unpaired fermions? A new possibility recently proposed is that unpaired fermions forming a Fermi sea smoothly change their character from atoms to triatomic molecules (trimers) with increasing the attraction [15]. At first glance, it may seem surprising and even impossible because an atom and trimer have different quantum numbers (particle numbers) and thus cannot be smoothly connected. However, because the condensation of Cooper pairs or molecules violates the particle number conservation in units of two, the atom and trimer are actually indistinguishable in a superfluid state and thus can be smoothly connected (see Fig. 1). This new type of crossover physics potentially emerging in three-component Fermi gases is termed an "atom-trimer continuity" in analogy with the "quark-hadron continuity" in a superfluid nuclear matter where deconfined quarks with three colors are considered to smoothly evolve into confined baryons with decreasing the nuclear density [16, 17].

The atom-trimer continuity was originally inspired by exploring the universal phase diagram of a three-component Fermi gas in the vicinity of a narrow Feshbach resonance [15]. It was found there by controlled analyses that the unpaired Fermi sea coexisting with condensed pairs is composed of atoms in the weak coupling dense limit while composed of trimers in the strong coupling dilute limit. Whether they are actually smoothly connected or not, however, still remains unestablished because of the lack of a unified theoretical framework

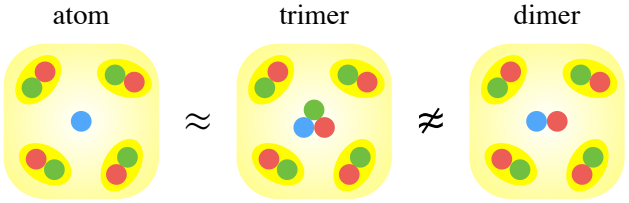

FIG. 1. Because of the presence of condensed pairs, atom (left) and trimer (middle) are indistinguishable in a superfluid state while they are still distinct from dimer (right).

that smoothly interpolates the above two limits. This difficulty largely originates from the fact that, unlike the BCS-BEC crossover for two-component Fermi gases, the ordinary mean-field approximation does not work for three-component Fermi gases because it completely misses three-body correlations playing an essential role here [15, 18–23]. Therefore, it is challenging but highly desired to develop a new crossover theory suitable for three-component Fermi gases. Important progress toward such a goal is to be made in this Letter by studying the corresponding polaron problem in which a single impurity atom of one component interacts with condensed pairs of the other two components of fermions with equal populations.

CROSSOVER WAVE FUNCTION

As emphasized in Ref. [15], the BCS-BEC crossover in two-component Fermi gases is often studied across a broad Feshbach resonance, where a three-component Fermi gas, however, does not have a universal many-body ground state because of the Thomas collapse [24]. A minimal extension to cure this problem is to consider a narrow Feshbach resonance which is characterized by the nonzero resonance range as well as the s-wave scattering length [25–28]. Assuming the same inter-component interaction for all possible three pairs [29, 30], the polaron problem of a three-component Fermi gas in the vicinity of a narrow Feshbach resonance is described by the two-channel Hamiltonian, $H = H_0 - \mu\,(N_1 + N_2)$, which consists of the canonical part

$$H_0 = \sum_{i=1,2,3}\sum_{\boldsymbol{p}}\left[\varepsilon_{\boldsymbol{p}}\,\psi_i^\dagger(\boldsymbol{p})\psi_i(\boldsymbol{p}) + \left(\frac{\varepsilon_{\boldsymbol{p}}}{2}+\nu\right)\phi_i^\dagger(\boldsymbol{p})\phi_i(\boldsymbol{p})\right] + \frac{g}{2\sqrt{V}}\sum_{i,j,k}\sum_{\boldsymbol{P},\boldsymbol{p}}\left[\epsilon_{ijk}\,\phi_i^\dagger(\boldsymbol{P})\psi_j(\boldsymbol{p})\psi_k(\boldsymbol{P}-\boldsymbol{p}) + \text{H.c.}\right] \tag{1}$$

with ϵ_{ijk} being the antisymmetric tensor and the particle number operator for the ith component of fermions:

$$N_i = \sum_{\boldsymbol{p}}\left[\psi_i^\dagger(\boldsymbol{p})\psi_i(\boldsymbol{p}) + \sum_{j\neq i}\phi_j^\dagger(\boldsymbol{p})\phi_j(\boldsymbol{p})\right]. \tag{2}$$

Here $\psi_i^\dagger(\boldsymbol{p})$ and $\phi_i^\dagger(\boldsymbol{p})$ with $i = 1, 2, 3$ create fermionic atoms and bosonic molecules with momentum $\boldsymbol{p}$ and obey the usual (anti)commutation relations, while $\varepsilon_{\boldsymbol{p}} \equiv \boldsymbol{p}^2/(2m)$ is the single-particle kinetic energy with the same mass m assumed for all three components of fermions. The chemical potential μ is introduced to only the first two components of fermions and chosen so that each component has the fixed particle number density of $n_1 = n_2 \equiv k_{\rm F}^3/(6\pi^2)$ in the thermodynamic limit $V \to \infty$. The bare detuning ν of a molecule ϕ_i and its coupling g to two atoms $\epsilon_{ijk}\psi_j\psi_k$ are related to the s-wave scattering length a and the resonance range R_* by

$$\frac{\nu}{g^2} = -\frac{m}{4\pi a} + \int_{|\boldsymbol{p}|<\Lambda}\frac{d\boldsymbol{p}}{(2\pi)^3}\frac{1}{2\varepsilon_{\boldsymbol{p}}} \tag{3}$$

and $g^2 = 4\pi/(m^2 R_*)$, where $\hbar = 1$ and the momentum cutoff Λ is sent to infinity at the end of calculations.

We now develop a variational approach aimed at a unified theoretical framework that smoothly interpolates the polaronic atom and trimer in a superfluid state. Because the first two components of fermions have equal populations and attract each other, they form Cooper pairs and condense. In order to describe them, we adopt the ordinary mean-field wave function

$$|\text{SF}\rangle = \exp\left[-\frac{|\lambda|^2}{2} + \lambda\phi_3^\dagger(\boldsymbol{0})\right]\prod_{\boldsymbol{p}}\left[u_{\boldsymbol{p}} + v_{\boldsymbol{p}}\psi_1^\dagger(\boldsymbol{p})\psi_2^\dagger(-\boldsymbol{p})\right]|0\rangle. \tag{4}$$

Here the variational parameters λ, $u_{\boldsymbol{p}}$, $v_{\boldsymbol{p}}$ are determined so as to minimize the energy expectation value $E_{\rm SF} \equiv \langle\text{SF}|H|\text{SF}\rangle$ under constraints $|u_{\boldsymbol{p}}|^2 + |v_{\boldsymbol{p}}|^2 = 1$ for all $\boldsymbol{p}$ to satisfy the normalization condition $\langle\text{SF}|\text{SF}\rangle = 1$. With the method of Lagrange multipliers, we find

$$|u_{\boldsymbol{p}}|^2 = \frac{E_{\boldsymbol{p}} + \varepsilon_{\boldsymbol{p}} - \mu}{2E_{\boldsymbol{p}}} \tag{5}$$

and $v_{\boldsymbol{p}} = \Delta/(2E_{\boldsymbol{p}}u_{\boldsymbol{p}}^*)$, where $E_{\boldsymbol{p}} \equiv \sqrt{(\varepsilon_{\boldsymbol{p}} - \mu)^2 + |\Delta|^2}$ is the quasiparticle energy and the gap parameter $\Delta \equiv g\lambda/\sqrt{V}$ as well as the chemical potential μ simultaneously solves the gap equation

$$-\frac{m}{4\pi a} - \frac{m^2 R_*\mu}{2\pi} = \int\frac{d\boldsymbol{p}}{(2\pi)^3}\left(\frac{1}{2E_{\boldsymbol{p}}} - \frac{1}{2\varepsilon_{\boldsymbol{p}}}\right) \tag{6a}$$

and the particle number density equation

$$\frac{k_{\rm F}^3}{6\pi^2} = \frac{m^2 R_*|\Delta|^2}{4\pi} + \int\frac{d\boldsymbol{p}}{(2\pi)^3}\frac{E_{\boldsymbol{p}} - \varepsilon_{\boldsymbol{p}} + \mu}{2E_{\boldsymbol{p}}}. \tag{6b}$$

These two coupled mean-field equations qualitatively describe the BCS-BEC crossover of the condensed pairs with increasing the attraction $1/ak_{\rm F}$ [31] and, furthermore, become exact in the narrow resonance limit $R_* k_{\rm F} \to \infty$ [32].

When a single impurity atom of the third component with momentum $\boldsymbol{k}$ is added to the above superfluid state (4), the simplest trial wave function to start with is

$$|\text{A}(\boldsymbol{k})\rangle = z_{\boldsymbol{k}}\psi_3^\dagger(\boldsymbol{k})|\text{SF}\rangle. \tag{7}$$

While this trial wave function seems to describe an atom-like impurity on top of the superfluid state, it can also be viewed as a trimer-like impurity at the same time because the particle number in the superfluid state fluctuates in

units of two. This peculiarity becomes evident by decomposing the superfluid wave function $|\mathrm{SF}\rangle$ in Eq. (7) into a superposition of fixed particle number wave functions:

$$|\mathrm{A}(\boldsymbol{k})\rangle \propto \sum_{N=0}^{\infty} \frac{\psi_3^\dagger(\boldsymbol{k})}{N!} \left[\Phi_3^\dagger(\boldsymbol{0})\right]^N |0\rangle \tag{8}$$

with the pair creation operator defined by

$$\Phi_3^\dagger(\boldsymbol{0}) \equiv \lambda\phi_3^\dagger(\boldsymbol{0}) + \sum_{\boldsymbol{p}} \frac{v_{\boldsymbol{p}}}{u_{\boldsymbol{p}}} \psi_1^\dagger(\boldsymbol{p})\psi_2^\dagger(-\boldsymbol{p}). \tag{9}$$

Here, if one state $\psi_3^\dagger(\boldsymbol{k})\left[\Phi_3^\dagger(\boldsymbol{0})\right]^N|0\rangle$ is viewed as the atom-like impurity, then another superposed state $\left[\psi_3^\dagger(\boldsymbol{k})\Phi_3^\dagger(\boldsymbol{0})\right]\left[\Phi_3^\dagger(\boldsymbol{0})\right]^N|0\rangle$ can be viewed as the trimer-like impurity in which the atom-like impurity is dressed by a zero-momentum pair extracted from the background condensate (see Fig. 1). In particular, because of the existence of the latter component in the atom-like wave function (7), it can hybridize with the following trimer-like wave function, i.e., $\langle \mathrm{A}(\boldsymbol{k})|H|\mathrm{T}(\boldsymbol{k})\rangle \neq 0$:

$$\begin{aligned}|\mathrm{T}(\boldsymbol{k})\rangle = \Bigg[&\frac{1}{\sqrt{V}} \sum_{\sigma=1,2} \sum_{\boldsymbol{p}} \alpha_{\boldsymbol{k}\sigma}(\boldsymbol{p}) \psi_\sigma^\dagger(\boldsymbol{p})\phi_\sigma^\dagger(\boldsymbol{k}-\boldsymbol{p}) \\ &+ \frac{1}{\sqrt{V}} \sum_{\boldsymbol{P}\neq\boldsymbol{0}} \psi_3^\dagger(\boldsymbol{k}-\boldsymbol{P}) \Bigg\{ \beta_{\boldsymbol{k}}(\boldsymbol{P})\phi_3^\dagger(\boldsymbol{P}) \\ &+ \frac{1}{\sqrt{V}} \sum_{\boldsymbol{p}} \gamma_{\boldsymbol{k}}(\boldsymbol{P},\boldsymbol{p}) \psi_1^\dagger(\boldsymbol{p})\psi_2^\dagger(\boldsymbol{P}-\boldsymbol{p}) \Bigg\} \Bigg] |\mathrm{SF}\rangle. \end{aligned} \tag{10}$$

This trimer-like wave function is constructed so that it becomes the most general three-body wave function in the zero density limit $|\mathrm{SF}\rangle \to |0\rangle$ and thus is capable of exactly reproducing the trimer formation in the vacuum. We note that the sum in the second line of Eq. (10) excludes $\boldsymbol{P} = \boldsymbol{0}$ because the corresponding component already exists in Eq. (7) as is evident from its decomposition (8) and, consequently, the above two wave functions have no overlap $\langle \mathrm{A}(\boldsymbol{k})|\mathrm{T}(\boldsymbol{k})\rangle = 0$. With all these preparations, we finally propose the ansatz

$$|\mathrm{AT}(\boldsymbol{k})\rangle = |\mathrm{A}(\boldsymbol{k})\rangle + |\mathrm{T}(\boldsymbol{k})\rangle \tag{11}$$

as a possible crossover wave function that smoothly interpolates atom-like $|\mathrm{A}(\boldsymbol{k})\rangle$ and trimer-like $|\mathrm{T}(\boldsymbol{k})\rangle$ impurities in a superfluid state and refer to it as a polaronic atom-trimer state.

At this point, it is worthwhile to contrast our polaronic atom-trimer state (11) with the usual polaron in a two-component Fermi gas [33, 34]. In the latter, a single impurity atom is dressed by a pair of particle and hole excited from the background Fermi sea [35, 36] and thus distinct from the trimer [37, 38], while in the former, a single impurity atom is dressed by a pair of two particles extracted from the background condensate and thus indistinguishable from the trimer. A similar situation can be found in Bose-Fermi mixtures where fermionic atoms and molecules are indistinguishable in the presence of condensed bosons [39–41]. In principle, the single impurity atom can be further dressed by two or more condensed pairs to form a pentamer-like or larger molecule, but their contributions to the impurity wave function are expected to be insignificant because their formations are not favored by the Pauli exclusion principle between the same component of fermions. We also note that our crossover wave function (11) differs in the spirit from the ansatz in Ref. [20] which is intended to describe the sharp transition from the superfluid phase to the trimer liquid phase.

POLARON PHASE DIAGRAM

The variational parameters $z_{\boldsymbol{k}}$, $\alpha_{\boldsymbol{k}\sigma}(\boldsymbol{p})$, $\beta_{\boldsymbol{k}}(\boldsymbol{P})$, $\gamma_{\boldsymbol{k}}(\boldsymbol{P},\boldsymbol{p})$ in the trial wave function (11) are determined so as to minimize its energy expectation value $\varepsilon_{\mathrm{AT}}(\boldsymbol{k}) \equiv \langle \mathrm{AT}(\boldsymbol{k})|H|\mathrm{AT}(\boldsymbol{k})\rangle - E_{\mathrm{SF}}$ under the normalization condition $\langle \mathrm{AT}(\boldsymbol{k})|\mathrm{AT}(\boldsymbol{k})\rangle = 1$. After straightforward calculations, we find that $\alpha_{\boldsymbol{k}}(\boldsymbol{p}) \equiv \alpha_{\boldsymbol{k}1}(\boldsymbol{p}) = \alpha_{\boldsymbol{k}2}(\boldsymbol{p})$ and $\beta_{\boldsymbol{k}}(\boldsymbol{P})$ simultaneously satisfy

$$\begin{aligned} &\left[-\frac{m}{4\pi a} + \frac{m^2 R_*}{4\pi} \left\{ \frac{\varepsilon_{\boldsymbol{k}-\boldsymbol{p}}}{2} - \mu + E_{\boldsymbol{p}} - \varepsilon_{\mathrm{AT}}(\boldsymbol{k}) \right\} \right. \\ &\left. - \int \frac{d\boldsymbol{P}}{(2\pi)^3} \left\{ \frac{|u_{\boldsymbol{P}-\boldsymbol{p}}|^2}{\varepsilon_{\boldsymbol{k}-\boldsymbol{P}} + E_{\boldsymbol{p}} + E_{\boldsymbol{P}-\boldsymbol{p}} - \varepsilon_{\mathrm{AT}}(\boldsymbol{k})} - \frac{1}{2\varepsilon_{\boldsymbol{p}}} \right\} \right] \alpha_{\boldsymbol{k}}(\boldsymbol{p}) \\ &= \frac{E_{\boldsymbol{p}} - \varepsilon_{\boldsymbol{p}} + \mu}{\varepsilon_{\boldsymbol{k}} - \varepsilon_{\mathrm{AT}}(\boldsymbol{k})} \int \frac{d\boldsymbol{q}}{(2\pi)^3} \frac{\alpha_{\boldsymbol{k}}(\boldsymbol{q})}{E_{\boldsymbol{q}}} \\ &\quad + \int \frac{d\boldsymbol{P}}{(2\pi)^3} \frac{|u_{\boldsymbol{P}-\boldsymbol{p}}|^2 \left[\alpha_{\boldsymbol{k}}(\boldsymbol{P}-\boldsymbol{p}) + \beta_{\boldsymbol{k}}(\boldsymbol{P})\right]}{\varepsilon_{\boldsymbol{k}-\boldsymbol{P}} + E_{\boldsymbol{p}} + E_{\boldsymbol{P}-\boldsymbol{p}} - \varepsilon_{\mathrm{AT}}(\boldsymbol{k})} \end{aligned} \tag{12a}$$

and

$$\begin{aligned} &\left[-\frac{m}{4\pi a} + \frac{m^2 R_*}{4\pi} \left\{ \varepsilon_{\boldsymbol{k}-\boldsymbol{P}} + \frac{\varepsilon_{\boldsymbol{P}}}{2} - 2\mu - \varepsilon_{\mathrm{AT}}(\boldsymbol{k}) \right\} \right. \\ &\left. - \int \frac{d\boldsymbol{p}}{(2\pi)^3} \left\{ \frac{|u_{\boldsymbol{p}}|^2 |u_{\boldsymbol{P}-\boldsymbol{p}}|^2}{\varepsilon_{\boldsymbol{k}-\boldsymbol{P}} + E_{\boldsymbol{p}} + E_{\boldsymbol{P}-\boldsymbol{p}} - \varepsilon_{\mathrm{AT}}(\boldsymbol{k})} - \frac{1}{2\varepsilon_{\boldsymbol{p}}} \right\} \right] \beta_{\boldsymbol{k}}(\boldsymbol{P}) \\ &= 2 \int \frac{d\boldsymbol{p}}{(2\pi)^3} \frac{|u_{\boldsymbol{p}}|^2 |u_{\boldsymbol{P}-\boldsymbol{p}}|^2 \alpha_{\boldsymbol{k}}(\boldsymbol{p})}{\varepsilon_{\boldsymbol{k}-\boldsymbol{P}} + E_{\boldsymbol{p}} + E_{\boldsymbol{P}-\boldsymbol{p}} - \varepsilon_{\mathrm{AT}}(\boldsymbol{k})}. \end{aligned} \tag{12b}$$

These two coupled integral equations have similar structures to the Skorniakov–Ter-Martirosian-type equations to determine the trimer binding energy in the vacuum [15], while the first term in the right-hand side of Eq. (12a) is the exception originating from the hybridization between the atom-like and trimer-like wave functions $\langle \mathrm{A}(\boldsymbol{k})|H|\mathrm{T}(\boldsymbol{k})\rangle \neq 0$ and thus plays an essential role here. By solving Eqs. (6) and (12) together with the normalization condition for a given set of inverse scattering length $1/ak_{\mathrm{F}}$ and resonance range $R_* k_{\mathrm{F}}$ [42], we obtain the quasiparticle energy $\varepsilon_{\mathrm{AT}}(\boldsymbol{k})$ and the normalized wave function $|\mathrm{AT}(\boldsymbol{k})\rangle$ of the polaronic atom-trimer state

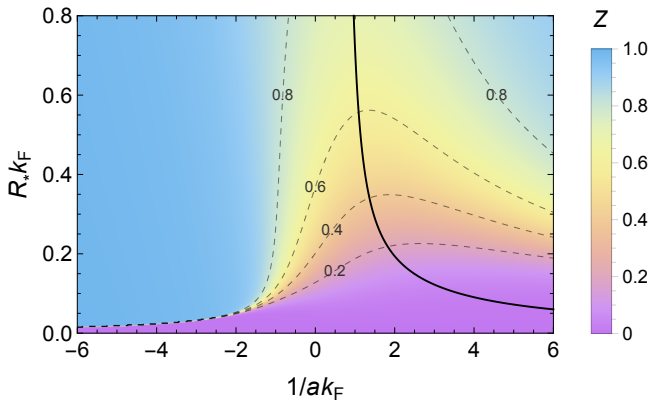

FIG. 2. Atomic fraction $Z \equiv |z_{\boldsymbol{k}=\boldsymbol{0}}|^2$ in the polaronic atom-trimer state (11) in the plane of the inverse scattering length $1/ak_\mathrm{F}$ and the resonance range R_*k_F. The impurity state is atom-like in the blue region ($Z \gtrsim 0.8$) while trimer-like in the purple region ($Z \lesssim 0.2$) and they are smoothly connected in the yellow-to-orange crossover region ($0.2 \lesssim Z \lesssim 0.8$). The black solid curve indicates the phase boundary above which the dimer state (15) has the lower energy than the polaronic atom-trimer state.

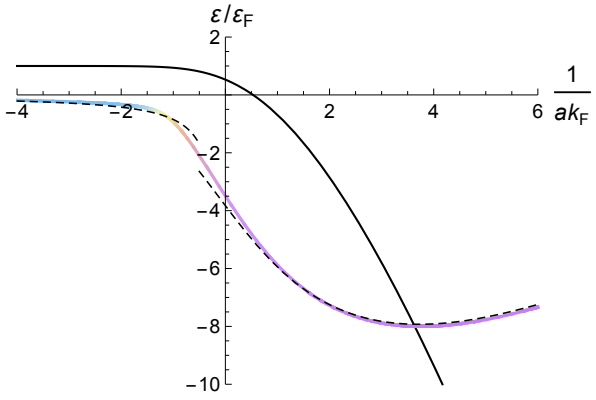

FIG. 3. Polaronic atom-trimer energy $\varepsilon_\mathrm{AT}(\boldsymbol{k}=\boldsymbol{0})$ in units of the Fermi energy $\varepsilon_\mathrm{F} \equiv k_\mathrm{F}^2/(2m)$ at $R_*k_\mathrm{F} = 0.1$ as a function of $1/ak_\mathrm{F}$. It is plotted by the colored solid curve with the atomic fraction Z indicated by the same color as in Fig. 2. The upper left dashed curve is the mean-field polaron energy $\varepsilon = (4\pi a/m)(k_\mathrm{F}^3/3\pi^2)$ [Eq. (13)] while the lower right one is the vacuum trimer binding energy $\varepsilon = E_3 - 2\mu$ [Eq. (14)]. The black solid curve represents the twofold degenerate dimer energy $\varepsilon_\mathrm{D}(\boldsymbol{0}) = \mu$ [Eq. (17)] obtained from the simple ansatz (15).

(11). In particular, the important quantity of our interest is the quasiparticle weight $|z_{\boldsymbol{k}}|^2 = \langle \mathrm{A}(\boldsymbol{k})|\mathrm{AT}(\boldsymbol{k})\rangle$, which measures the atomic fraction contained in the impurity wave function while the rest $1 - |z_{\boldsymbol{k}}|^2 = \langle \mathrm{T}(\boldsymbol{k})|\mathrm{AT}(\boldsymbol{k})\rangle$ measures the trimeric fraction therein. Therefore, it can serve as an indicator of the polaronic atom-trimer continuity.

Figure 2 shows the numerically obtained atomic fraction $Z \equiv |z_{\boldsymbol{0}}|^2$ assuming zero center-of-mass momentum $\boldsymbol{k} = \boldsymbol{0}$ as well as zero orbital angular momentum, i.e., $\alpha_{\boldsymbol{0}}(\boldsymbol{p}) = \alpha_{\boldsymbol{0}}(|\boldsymbol{p}|)$ and $\beta_{\boldsymbol{0}}(\boldsymbol{P}) = \beta_{\boldsymbol{0}}(|\boldsymbol{P}|)$, where the polaronic atom-trimer state is expected to have the lowest energy. In the plane of $1/ak_\mathrm{F}$ and R_*k_F, we find that the impurity state is atom-like $Z \sim 1$ in the weak coupling (small $1/ak_\mathrm{F}$) or narrow resonance (large R_*k_F) region while it becomes trimer-like $Z \sim 0$ toward the strong coupling (large $1/ak_\mathrm{F}$) and broad resonance (small R_*k_F) region. These two regions are indeed smoothly connected in between and thus exhibit the polaronic atom-trimer continuity. We note that this smooth crossover from the atom-like impurity to the trimer-like impurity becomes increasingly sharper toward the weak coupling and broad resonance limit, $1/ak_\mathrm{F} \to -\infty$ and $R_*k_\mathrm{F} \to 0$, which is equivalent to taking the zero density limit $k_\mathrm{F} \to 0$ and thus the phase boundary there coincides with the threshold $R_*/a = -0.0917249$ for the trimer formation in the vacuum [15].

The polaronic atom-trimer continuity is also exhibited by the quasiparticle energy $\varepsilon_\mathrm{AT}(\boldsymbol{0})$ of the polaronic atom-trimer state (11). In the weak coupling limit $1/ak_\mathrm{F} \to -\infty$ where the impurity state is atom-like $Z \to 1$, its energy resulting from Eqs. (12) reduces to the usual mean-field polaron energy [36]

$$\varepsilon_\mathrm{AT}(\boldsymbol{0}) \to \frac{4\pi a}{m}(n_1 + n_2)\,. \tag{13}$$

On the other hand, in the broad resonance limit $R_*k_\mathrm{F} \to 0$ where the impurity state is trimer-like $Z \to 0$, its energy resulting from Eqs. (12) can be expressed in terms of the trimer binding energy E_3 in the vacuum [43] as

$$\varepsilon_\mathrm{AT}(\boldsymbol{0}) \to E_3 - 2\mu. \tag{14}$$

These two asymptotic formulas as well as the numerically obtained polaronic atom-trimer energy $\varepsilon_\mathrm{AT}(\boldsymbol{0})$ are plotted in Fig. 3 as functions of $1/ak_\mathrm{F}$ by choosing $R_*k_\mathrm{F} = 0.1$ for demonstration. Here we find that the mean-field polaron energy (13) valid in the atom-like region ($1/ak_\mathrm{F} \lesssim -1$) and the vacuum trimer binding energy (14) valid in the trimer-like region ($1/ak_\mathrm{F} \gtrsim 0$) are indeed smoothly interpolated by the polaronic atom-trimer energy $\varepsilon_\mathrm{AT}(\boldsymbol{0})$ and thus we again confirm the polaronic atom-trimer continuity.

So far we have considered that a single impurity atom of the third component binds two fermions from a superfluid state of the other two components to form a trimer-like impurity. On the other hand, there exists another possibility in which the single impurity atom binds one fermion to form a dimer-like impurity and becomes distinct from the above polaronic atom-trimer state (see Fig. 1). Such a dimer state is twofold degenerate with respect to the exchange of components $1 \leftrightarrow 2$ and the

simplest trial wave function to describe one of the two is

$$|\mathrm{D}(\boldsymbol{k})\rangle = \left[\bar{\beta}_{\boldsymbol{k}}\phi_1^\dagger(\boldsymbol{k}) + \frac{1}{\sqrt{V}}\sum_{\boldsymbol{p}}\bar{\gamma}_{\boldsymbol{k}}(\boldsymbol{p})\psi_2^\dagger(\boldsymbol{p})\psi_3^\dagger(\boldsymbol{k}-\boldsymbol{p})\right]|\mathrm{SF}\rangle. \tag{15}$$

By minimizing its energy expectation value $\varepsilon_{\mathrm{D}}(\boldsymbol{k}) \equiv \langle \mathrm{D}(\boldsymbol{k})|H|\mathrm{D}(\boldsymbol{k})\rangle - E_{\mathrm{SF}}$ with respect to the variational parameters $\bar{\beta}_{\boldsymbol{k}}$, $\bar{\gamma}_{\boldsymbol{k}}(\boldsymbol{p})$ under the normalization condition $\langle \mathrm{D}(\boldsymbol{k})|\mathrm{D}(\boldsymbol{k})\rangle = 1$ [44], we obtain an equation solved by $\varepsilon_{\mathrm{D}}(\boldsymbol{k})$:

$$\begin{aligned} &-\frac{m}{4\pi a} + \frac{m^2 R_*}{4\pi}\left[\frac{\varepsilon_{\boldsymbol{k}}}{2} - \mu - \varepsilon_{\mathrm{D}}(\boldsymbol{k})\right] \\ &= \int \frac{d\boldsymbol{p}}{(2\pi)^3}\left[\frac{|u_{\boldsymbol{p}}|^2}{E_{\boldsymbol{p}} + \varepsilon_{\boldsymbol{k}-\boldsymbol{p}} - \varepsilon_{\mathrm{D}}(\boldsymbol{k})} - \frac{1}{2\varepsilon_{\boldsymbol{p}}}\right]. \end{aligned} \tag{16}$$

In particular, by comparing Eq. (16) with the gap equation (6a), its solution at zero center-of-mass momentum $\boldsymbol{k} = \boldsymbol{0}$ is easily identified as

$$\varepsilon_{\mathrm{D}}(\boldsymbol{0}) = \mu. \tag{17}$$

The resulting dimer energy at $R_* k_{\mathrm{F}} = 0.1$ is also plotted in Fig. 3 where we find that the twofold degenerate dimer states have the lower energy than the polaronic atom-trimer state in the strong coupling region $1/ak_{\mathrm{F}} > 3.6$. Therefore, in addition to the above smooth crossover from the atom-like impurity to the trimer-like impurity, there is a sharp transition to the dimer-like impurity with increasing the attraction $1/ak_{\mathrm{F}}$ and the corresponding phase boundary in the plane of $1/ak_{\mathrm{F}}$ and $R_* k_{\mathrm{F}}$ is indicated in Fig. 2. This sharp transition from the polaronic atom-trimer state (11) to the dimer state (15) is indeed a close analog of the polaron-molecule transition in a two-component Fermi gas [45].

SUMMARY AND OUTLOOK

This Letter is aimed at developing a new crossover theory that smoothly interpolates atom and trimer in three-component Fermi gases. To this end, we took a variational approach in the vicinity of a narrow Feshbach resonance and successfully showed that a single impurity atom in the presence of condensed pairs smoothly changes its character from atom to trimer with increasing the attraction and eventually there is a sharp transition to dimer. The emergent polaronic atom-trimer continuity is signaled by the rapid decrease of the quasiparticle weight $|z_{\boldsymbol{k}}|^2$ as well as the polaron energy $\varepsilon_{\mathrm{AT}}(\boldsymbol{k})$ evolving into the trimer binding energy (see Fig. 3 for $\boldsymbol{k} = \boldsymbol{0}$). These key quantities are actually measurable in ultracold atom experiments by transferring an impurity atom with momentum $\boldsymbol{k}$ from a non-interacting state to an interacting state, whose transition rate at frequency ω exhibits a quasiparticle peak of [46–49]

$$I_{\boldsymbol{k}}(\omega)|_{\mathrm{peak}} = |z_{\boldsymbol{k}}|^2\delta[\omega + \varepsilon_{\boldsymbol{k}} - \varepsilon_{\mathrm{AT}}(\boldsymbol{k})]. \tag{18}$$

Therefore, by utilizing this inverse radio-frequency or microwave spectroscopy [50, 51], the polaronic atom-trimer continuity may be experimentally probed, for example, with a three-component Fermi gas of ^{6}Li [7–9] or a recently realized superfluid Bose-Fermi mixture of ^{7}Li-^{6}Li [52].

Our findings on the polaron problem also have immediate consequences on the phase diagram of a three-component Fermi gas with a small concentration $n_3 \ll n_1 = n_2$ introduced to the third component of fermions. When the polaronic atom-trimer state (11) is the ground state, it will form an unpaired Fermi sea coexisting with the condensed pairs of the other two components. Because its many-body wave function is provided by

$$|\mathrm{FS}\rangle_{\mathrm{AT}} = \prod_{\varepsilon_{\mathrm{AT}}(\boldsymbol{k})<\mu_3}\Psi_3^\dagger(\boldsymbol{k})|\mathrm{SF}\rangle \tag{19}$$

with $\Psi_3^\dagger(\boldsymbol{k})$ being the creation operator of a single atom-trimer state $\Psi_3^\dagger(\boldsymbol{k})|\mathrm{SF}\rangle \equiv |\mathrm{AT}(\boldsymbol{k})\rangle$, the unpaired Fermi sea of atoms smoothly evolves into that of trimers with Fig. 2 scanned from the upper left region to the lower region. On the other hand, when the twofold degenerate dimer states (15) are the ground state, they will undergo the Bose-Einstein condensation and thus the three different pair condensates coexist with no unpaired fermions in the upper right side of the phase boundary in Fig. 2. It is impressive to find that the polaron phase diagram obtained here is already similar in essential features to the schematic phase diagram proposed in the case of equal populations for all three components of fermions [15]. Our novel crossover wave function (11) properly incorporating the polaronic atom-trimer continuity, as well as the dimer wave function (15), will provide a useful basis to further investigate the phase diagram of three-component Fermi gases in more general situations, including unequal masses, populations, and inter-component interactions, relevant to ultracold atom experiments [7–9, 52].

This work was supported by JSPS KAKENHI Grant Number 25887020. Part of the numerical calculations were carried out at the YITP computer facility in Kyoto University.

[1] D. M. Eagles, Phys. Rev. **186**, 456 (1969).
[2] A. J. Leggett, *Modern Trends in the Theory of Condensed Matter,* edited by A. Pekalski and R. Przystawa (Springer-Verlag, Berlin, 1980); J. Phys. (Paris), Colloq. **41**, C7 (1980).
[3] See, for example, *The BCS-BEC Crossover and the Unitary Fermi Gas,* Lecture Notes in Physics, Vol. 836, edited by Z. Wilhelm (Springer-Verlag, Berlin, 2012).

[4] C. A. Regal, M. Greiner, and D. S. Jin, Phys. Rev. Lett. **92**, 040403 (2004).

[5] M. W. Zwierlein, C. A. Stan, C. H. Schunck, S. M. F. Raupach, A. J. Kerman, and W. Ketterle, Phys. Rev. Lett. **92**, 120403 (2004).

[6] See, also, *Ultracold Fermi Gases,* Proceedings of the International School of Physics "Enrico Fermi," Course CLXIV, edited by M. Inguscio, W. Ketterle, and C. Salomon (IOS Press, Amsterdam, 2008).

[7] T. B. Ottenstein, T. Lompe, M. Kohnen, A. N. Wenz, and S. Jochim, Phys. Rev. Lett. **101**, 203202 (2008); A. N. Wenz, T. Lompe, T. B. Ottenstein, F. Serwane, G. Zürn, and S. Jochim, Phys. Rev. A **80**, 040702(R) (2009); T. Lompe, T. B. Ottenstein, F. Serwane, K. Viering, A. N. Wenz, G. Zürn, and S. Jochim, Phys. Rev. Lett. **105**, 103201 (2010); T. Lompe, T. B. Ottenstein, F. Serwane, A. N. Wenz, G. Zürn, and S. Jochim, Science **330**, 940 (2010).

[8] J. H. Huckans, J. R. Williams, E. L. Hazlett, R. W. Stites, and K. M. O'Hara, Phys. Rev. Lett. **102**, 165302 (2009); J. R. Williams, E. L. Hazlett, J. H. Huckans, R. W. Stites, Y. Zhang, and K. M. O'Hara, Phys. Rev. Lett. **103**, 130404 (2009).

[9] S. Nakajima, M. Horikoshi, T. Mukaiyama, P. Naidon, and M. Ueda, Phys. Rev. Lett. **105**, 023201 (2010); Phys. Rev. Lett. **106**, 143201 (2011).

[10] C. Honerkamp and W. Hofstetter, Phys. Rev. Lett. **92**, 170403 (2004); Phys. Rev. B **70**, 094521 (2004).

[11] T. Paananen, J.-P. Martikainen, and P. Törmä, Phys. Rev. A **73**, 053606 (2006).

[12] L. He, M. Jin, and P. Zhuang, Phys. Rev. A **74**, 033604 (2006).

[13] R. W. Cherng, G. Refael, and E. Demler, Phys. Rev. Lett. **99**, 130406 (2007).

[14] If the system is SU(3) symmetric, i.e., all three components have the same mass, population, and intercomponent interaction, all possible three pairs are formed with the same amplitude ($\Delta_{12} = \Delta_{23} = \Delta_{31}$) while an equal superposition of the three components ($|1\rangle + |2\rangle + |3\rangle$) forms an unpaired Fermi sea [12, 15]. Therefore, the spontaneous population imbalance and the resulting domain formation sometimes discussed in the literature do not take place because of its surface energy cost compared to the above uniform state.

[15] Y. Nishida, Phys. Rev. Lett. **109**, 240401 (2012).

[16] T. Schäfer and F. Wilczek, Phys. Rev. Lett. **82**, 3956 (1999).

[17] See, also, F. Wilczek, Nat. Phys. **3**, 375 (2007).

[18] P. F. Bedaque and J. P. D'Incao, Ann. Phys. (Amsterdam) **324**, 1763 (2009).

[19] S. Y. Chang and V. R. Pandharipande, arXiv:physics/0607008 [physics.atom-ph].

[20] Á. Rapp, G. Zaránd, C. Honerkamp, and W. Hofstetter, Phys. Rev. Lett. **98**, 160405 (2007); Á. Rapp, W. Hofstetter, and G. Zaránd, Phys. Rev. B **77**, 144520 (2008).

[21] S. Floerchinger, R. Schmidt, S. Moroz, and C. Wetterich, Phys. Rev. A **79**, 013603 (2009).

[22] P. Niemann and H.-W. Hammer, Phys. Rev. A **86**, 013628 (2012).

[23] N. G. Nygaard and N. T. Zinner, New J. Phys. **16**, 023026 (2014); N. T. Zinner, Few-Body Syst. **55**, 599 (2014).

[24] L. H. Thomas, Phys. Rev. **47**, 903 (1935).

[25] D. S. Petrov, Phys. Rev. Lett. **93**, 143201 (2004).

[26] A. O. Gogolin, C. Mora, and R. Egger, Phys. Rev. Lett. **100**, 140404 (2008).

[27] L. Pricoupenko, Phys. Rev. Lett. **110**, 180402 (2013).

[28] E. L. Hazlett, Y. Zhang, R. W. Stites, and K. M. O'Hara, Phys. Rev. Lett. **108**, 045304 (2012).

[29] P. Zhang, P. Naidon, and M. Ueda, Phys. Rev. Lett. **103**, 133202 (2009).

[30] K. M. O'Hara, New J. Phys. **13**, 065011 (2011).

[31] The integrals in Eqs. (6) can be expressed in terms of the complete elliptic integrals of the first and second kind. See, M. Marini, F. Pistolesi, and G. C. Strinati, Eur. Phys. J. **1**, 151 (1998).

[32] V. Gurarie and L. Radzihovsky, Ann. Phys. (Amsterdam) **322**, 2 (2007).

[33] A. Schirotzek, C.-H. Wu, A. Sommer, and M. W. Zwierlein, Phys. Rev. Lett. **102**, 230402 (2009).

[34] See, also, P. Massignan, M. Zaccanti, and G. Bruun, Rep. Prog. Phys. **77**, 034401 (2014).

[35] F. Chevy, Phys. Rev. A **74**, 063628 (2006).

[36] R. Combescot, A. Recati, C. Lobo, and F. Chevy, Phys. Rev. Lett. **98**, 180402 (2007).

[37] C. J. M. Mathy, M. M. Parish, and D. A. Huse, Phys. Rev. Lett. **106**, 166404 (2011).

[38] M. M. Parish and J. Levinsen, Phys. Rev. A **87**, 033616 (2013).

[39] S. Powell, S. Sachdev, and H. P. Büchler, Phys. Rev. B **72**, 024534 (2005).

[40] F. M. Marchetti, C. J. M. Mathy, D. A. Huse, and M. M. Parish, Phys. Rev. B **78**, 134517 (2008).

[41] S. P. Rath and R. Schmidt, Phys. Rev. A **88**, 053632 (2013).

[42] Once the solutions $\alpha_{\boldsymbol{k}}(\boldsymbol{p})$ and $\beta_{\boldsymbol{k}}(\boldsymbol{P})$ are obtained from Eqs. (12), the other two parameters are determined by

$$z_{\boldsymbol{k}} = \frac{g\Delta^*}{\varepsilon_{\boldsymbol{k}} - \varepsilon_{\rm AT}(\boldsymbol{k})} \int \frac{d\boldsymbol{q}}{(2\pi)^3} \frac{\alpha_{\boldsymbol{k}}(\boldsymbol{q})}{E_{\boldsymbol{q}}}$$

and

$$\gamma_{\boldsymbol{k}}(\boldsymbol{P},\boldsymbol{p}) = g\, \frac{\alpha_{\boldsymbol{k}}(\boldsymbol{p}) + \alpha_{\boldsymbol{k}}(\boldsymbol{P}-\boldsymbol{p}) + \beta_{\boldsymbol{k}}(\boldsymbol{P})}{\varepsilon_{\boldsymbol{k}-\boldsymbol{P}} + E_{\boldsymbol{p}} + E_{\boldsymbol{P}-\boldsymbol{p}} - \varepsilon_{\rm AT}(\boldsymbol{k})},$$

which have to be normalized according to

$$|z_{\boldsymbol{k}}|^2 + 2\int \frac{d\boldsymbol{p}}{(2\pi)^3} |u_{\boldsymbol{p}}|^2 |\alpha_{\boldsymbol{k}}(\boldsymbol{p})|^2 + \int \frac{d\boldsymbol{P}}{(2\pi)^3} |\beta_{\boldsymbol{k}}(\boldsymbol{P})|^2 + \iint \frac{d\boldsymbol{P} d\boldsymbol{p}}{(2\pi)^6} |u_{\boldsymbol{p}}|^2 |u_{\boldsymbol{P}-\boldsymbol{p}}|^2 |\gamma_{\boldsymbol{k}}(\boldsymbol{P},\boldsymbol{p})|^2 = 1.$$

[43] For a plot of the trimer binding energy E_3 in the vacuum as a function of R_*/a, see Fig. 2 in Y. Nishida, arXiv:1207.6971 [cond-mat.quant-gas].

[44] The normalized solutions are found to be

$$|\bar{\beta}_{\boldsymbol{k}}|^2 = \left[1 + g^2 \int \frac{d\boldsymbol{p}}{(2\pi)^3} \frac{|u_{\boldsymbol{p}}|^2}{[E_{\boldsymbol{p}} + \varepsilon_{\boldsymbol{k}-\boldsymbol{p}} - \varepsilon_{\rm D}(\boldsymbol{k})]^2}\right]^{-1}$$

and $\bar{\gamma}_{\boldsymbol{k}}(\boldsymbol{p}) = g\bar{\beta}_{\boldsymbol{k}}/[E_{\boldsymbol{p}} + \varepsilon_{\boldsymbol{k}-\boldsymbol{p}} - \varepsilon_{\rm D}(\boldsymbol{k})]$.

[45] N. V. Prokof'ev and B. V. Svistunov, Phys. Rev. B **77**, 020408(R) (2008); Phys. Rev. B **77**, 125101 (2008).

[46] P. Massignan and G. M. Bruun, Eur. Phys. J. D **65**, 83 (2011).

[47] R. Schmidt and T. Enss, Phys. Rev. A **83**, 063620 (2011).

[48] R. Schmidt, T. Enss, V. Pietilä, and E. Demler, Phys. Rev. A **85**, 021602(R) (2012).

[49] A. Shashi, F. Grusdt, D. A. Abanin, and E. Demler, Phys. Rev. A **89**, 053617 (2014).

[50] B. Fröhlich, M. Feld, E. Vogt, M. Koschorreck, W. Zwerger, and M. Köhl, Phys. Rev. Lett. **106**, 105301 (2011); M. Koschorreck, D. Pertot, E. Vogt, B. Fröhlich, M. Feld, and M. Köhl, Nature (London) **485**, 619 (2012).

[51] C. Kohstall, M. Zaccanti, M. Jag, A. Trenkwalder, P. Massignan, G. M. Bruun, F. Schreck, and R. Grimm, Nature (London) **485**, 615 (2012).

[52] I. Ferrier-Barbut, M. Delehaye, S. Laurent, A. T. Grier, M. Pierce, B. S. Rem, F. Chevy, and C. Salomon, Science **345**, 1035 (2014).